Water Air Soil Pollut (2011) 215:449–464
DOI 10.1007/s11270-010-0490-1

Sorption of Selected Aromatic Substances—Application of Kinetic Concepts and Quantum Mechanical Modeling

Sabine Klepsch · Adelia J. A. Aquino · Ursula Haas · Daniel Tunega · Georg Haberhauer · Martin H. Gerzabek · Hans Lischka

Received: 3 March 2010 / Accepted: 18 May 2010 / Published online: 5 June 2010

Abstract Prediction of the sorption behavior of environmental pollutants is of utmost importance within the framework of risk assessments. In this work two approaches are presented with the aim to describe sorption of aromatic substances to geosorbents. First, analytical solutions of kinetic models were fitted to experimental data of batch sorption experiments with aniline and 1-naphthylamine onto animal manure-treated soil and the soil mineral montmorillonite. The models, accounting for equilibrium and nonequilibrium sorption coupled to transformation and/or irreversible sorption processes, could well reproduce the concentration course of the sorbates. Results suggest that the amounts transformed/degraded and irreversibly bound were higher for the soil than for the clay mineral. In the second part, quantum chemical calculations were performed on aniline and 1-naphthylamine interacting with acetic acid, acetamide, imidazole, and phenol as models of functional groups present in humic substances. Molecular modeling showed that formation of hydrogen bonds is the dominating binding mechanism in all modeled complexes, which are energetically very similar between aniline and 1-naphthylamine.

Keywords Kinetic sorption processes · Mathematical modeling · Analytical solutions · Quantum chemical modeling

S. Klepsch (✉) · A. J. A. Aquino (✉) · D. Tunega · M. H. Gerzabek
Institute of Soil Research, University of Natural Resources and Applied Life Sciences,
Peter-Jordan-Straße 82b,
1190 Vienna, Austria
e-mail: sabine.klepsch@boku.ac.at
e-mail: adelia.aquino@univie.ac.at

S. Klepsch · U. Haas · G. Haberhauer
Health and Environment Department, AIT Austrian Institute of Technology,
A-2444 Seibersdorf, Austria

A. J. A. Aquino · D. Tunega · H. Lischka
Institute for Theoretical Chemistry, University of Vienna,
Währingerstraße 17,
1090 Vienna, Austria

1 Introduction

Many aromatic compounds are known as environmental pollutants, since they are widely used as synthetic intermediates in the industry for the manufacturing of dyestuffs, pesticides, rubbers, adhesives, plastics, and pharmaceuticals or utilized as antioxidant additives for industrial or engine lubricants (Vogt and Geralis 1985). Their application represents potential risk for natural waters and soils. Soil is an intricate entity holding huge portions of organic and inorganic (mineral) constituents onto which molecules can adsorb and be prevented from leaching to

groundwater. The term soil organic matter (SOM) is commonly used to characterize the organic components in soils, including high molecular weight organic materials, for example polysaccharides and proteins, small substances such as sugars and amino acids, as well as humic substances (HS). The reactivity of the latter is based on their functional group chemistry and microstructure, which are in sequence influenced by the composition of the nearby media. HS symbolize key organic components actively partaking in sorption processes (Kile et al. 1999). They proceed as surprise attacks for pollutants mostly via surface functional groups or binding in cavity-like sorption sites (Ghabbour and Davis 2000). Owing to the structural complexity of the HS, a large number of interactions, like hydrogen bonding, cation bridges, anion and cation exchange, ligand exchange, and van der Waals and hydrophobic interactions have been observed for them. In addition to physical interactions, functional groups can undergo chemical reactions with other compounds like pesticides that can lead to the formation of bound residues (Gevao et al. 2000).

It has been illustrated that also inorganic soil components like soil minerals (various clays, oxides, hydroxides, and oxy-hydroxides) have a considerable impact on the sorption properties of various species (Parker and Rae 1998; Dixon and Schulze 2002). Especially in soils with low organic matter content (less than a few tenths of a percent), sorption to mineral surfaces becomes important or dominant (Pignatello 1989; Schwarzenbach and Westall 1981). Two principal types of mineral surfaces exist, a strongly hydrophilic, hydroxylated surface of varying charge consisting of –OH groups protruding into solution from topmost layer of metal ions, and a siloxane surface consisting of oxygen atoms bridging underlying Si^{4+} ions (Pignatello 2000). The latter surface type can have a permanent negative charge due to isomorphic substitutions of central cations (e.g., Al^{3+} for Si^{4+}), with a strong hydrophilic surface in the vicinity of the charge, whereas the neutral regions between charges are hydrophobic or only weakly hydrophilic.

Sorption experiments with organic substances (Karickhoff 1980; Brusseau et al. 1991; Nkedi-Kizza et al. 2006) show that the process of adsorption often cannot be described with pure equilibrium models such as sorption isotherms but that kinetic concepts have to be applied to interpret the data. For example, with regard to primary amines binding to humate in a rapid and slow phase, initiation of a slow and irreversible covalent binding process by 1,4-nucleophilic addition via the amino group to quinone-like structures (present in humic matter) has been assumed, followed by rapid tautomerization and oxidation to form aminoquinones (Parris 1980; Weber et al. 1996). The time to approach the state of sorption equilibrium might range from days to weeks (Karickhoff and Morris 1985), months, or even years (Delle Site 2001), depending on the chemical properties of a particular sorbate and sorbent but also on parameters such as temperature, humidity, pH, and ionic strength. Batch sorption studies enable mathematical analysis of experimental data producing kinetic parameters and equilibrium adsorption values (for time $(t)\rightarrow\infty$) using appropriate nonequilibrium models.

In this work, the applicability of several semi-mechanistic kinetic models, based on the widely used biphasic sorption concepts and extended with terms for decay and/or irreversible sorption, is investigated in order to determine the long-term sorption behavior of two aromatic amines, 1-naphthylamine (NA), and aniline (AN). Sorbents were animal manure-treated soil (AM) and Ca^{2+}-saturated montmorillonite (MONTM), respectively.

Kinetic concepts have been numerously reviewed and applied to simulate sorption processes (Sparks 1989; Pignatello 1989; Ho 2006). While the equations were often solved numerically, we present analytical solutions for selected models.

Additionally, quantum chemical calculations have been performed aiming at modeling of molecular interactions occurring in sorption processes on HS. A comprehensive modeling of adsorption processes in soil systems at a quantum chemical level is not fully possible due to the large complexity of such processes. Taking this into account, the molecular models developed in this work aim at hydrogen-bonded interactions of specific organic sorbents containing relevant functional groups occurring in HS with AN and NA, respectively, with the aim of obtaining interesting information on the role of hydrogen bonding for the adsorption processes studied allowing conclusions about their role in explaining differences in the adsorption behavior of the two selected adsorbates.

2 Methods

2.1 Kinetic Sorption Models

2.1.1 Two-Site Kinetic Model

One of the applied mathematical concepts is the widely used two-site model (TSM) for calculating sorption nonequilibrium with the diffusion/dispersion and convective term set equal zero. For this model two sorbate phases, one calculating equilibrium sorption (type 1) and the other first-order kinetics (type 2), are assumed (Selim et al. 1976):

$$\left(1+\frac{f\rho K_\mathrm{d}}{\theta}\right)\frac{\mathrm{d}c(t)}{\mathrm{d}t}+\frac{\rho}{\theta}\frac{\mathrm{d}s_2(t)}{\mathrm{d}t}=0 \tag{1}$$

$$\frac{\mathrm{d}s_2(t)}{\mathrm{d}t}=\omega[(1-f)K_\mathrm{d}c(t)-s_2(t)] \tag{2}$$

where c(t)=solution concentration (milligram per liter), ρ=mass of soil (in grams regarding batch experiments; for porous media, bulk density), θ=volume of water (in milliliter regarding batch experiments; for porous media, volumetric water content), K_d=distribution constant for equilibrium sorption (milliliter per gram; equilibrium sorption is modeled with a Henry-type isotherm, $s_1(t)=fK_\mathrm{d}c(t)$, leading to the second term of the left-hand side of Eq. 1, $s_2(t)$=sorbed concentration (type-2 sites, in milligram per kilogram), ω=first-order rate coefficient (per hour), and f=fraction of all sites occupied by type-1 sorption sites (dimensionless). The total sorbed concentration at equilibrium ($t\rightarrow\infty$) is $s=s_1+s_2=K_\mathrm{d}c$.

The mathematical solution of Eqs. 1 and 2 is analogous to the work by Nkedi-Kizza et al. (2006) with the difference that they implemented forward and backward reactions ($k_{+/-}$) for the mass transfer reaction in the two-site model, instead of using a transfer rate as in Eq. 2:

$$\mathrm{c}\leftrightarrow \mathrm{S}_1 \underset{k_-}{\overset{k_+}{\rightleftarrows}} \mathrm{S}_2$$

Equation 2 combined with the mass balance Eq. 1 results in

$$\left(1+\frac{f\rho K_\mathrm{d}}{\theta}\right)\frac{\mathrm{d}c(t)}{\mathrm{d}t}+\frac{\rho}{\theta}\omega[(1-f)K_\mathrm{d}c(t)-s_2(t)]=0 \tag{3}$$

and rearranged for $\rho\cdot s_2$

$$\rho\cdot s_2(t)=\frac{\theta}{\omega}\cdot\left(1+\frac{\rho}{\theta}\cdot f\cdot K_\mathrm{d}\right)\frac{\mathrm{d}c(t)}{\mathrm{d}t}+\rho\cdot(1-f)\cdot K_\mathrm{d}\cdot c(t). \tag{4}$$

Since with the above assumption of no decay, the total concentration (in liquid and adsorbed phase) must not change during the batch experiment (c_in= input concentration),

$$\begin{aligned}\theta\cdot c_\mathrm{in}&=\theta\cdot c(t)+\rho\cdot(s_1(t)+s_2(t))\\&=c(t)\cdot(\theta+f\cdot\rho\cdot K_\mathrm{d})+\rho\cdot s_2(t).\end{aligned} \tag{5}$$

s_2, from Eq. 5, inserted into Eq. 4, results in

$$\begin{aligned}&\tfrac{\mathrm{d}c(t)}{\mathrm{d}t}\cdot\left[\tfrac{\theta}{\omega}\left(1+\tfrac{\rho}{\theta}\cdot f\cdot K_\mathrm{d}\right)\right]+\rho\cdot(1-f)\cdot K_\mathrm{d}\cdot c(t)\\&\quad+(\theta+\rho\cdot f\cdot K_\mathrm{d})\cdot c(t)=\theta\cdot c_\mathrm{in},\\&\text{or }\tfrac{\mathrm{d}c(t)}{\mathrm{d}t}+c(t)\cdot\tfrac{\omega}{\theta}\left[\tfrac{\rho(1-f)K_\mathrm{d}}{\left(1+\frac{\rho}{\theta}f\cdot K_\mathrm{d}\right)}+\theta\right]-\tfrac{\omega c_\mathrm{in}}{\left(1+\frac{\rho}{\theta}f\cdot K_\mathrm{d}\right)}=0.\end{aligned} \tag{6}$$

The analytical solution of Eq. 6 is

$$c(t)=\frac{\omega\cdot c_\mathrm{in}}{k\cdot\left(1+\frac{\rho}{\theta}\cdot f\cdot K_\mathrm{d}\right)}+\mathrm{e}^{-kt}\cdot\left(c_0-\frac{\omega\cdot c_\mathrm{in}}{k\cdot\left(1+\frac{\rho}{\theta}\cdot f\cdot K_\mathrm{d}\right)}\right)\text{ or} \tag{7}$$

$$c(t)=\frac{\omega}{k}\cdot c_0+\mathrm{e}^{-kt}\cdot c_0\cdot\left(1-\frac{\omega}{k}\right), \tag{8}$$

with the rate $k=\omega\cdot\left(\frac{\rho\cdot(1-f)\cdot K_\mathrm{d}}{(\theta+\rho\cdot f\cdot K_\mathrm{d})}+1\right)=\omega\cdot\left(\frac{\theta+\rho\cdot K_\mathrm{d}}{\theta+\rho\cdot f\cdot K_\mathrm{d}}\right)$ and the concentration c_0, arising directly after c_in has been added to the system, due to the instantaneous sorption reaction (s_1), $c_0=\frac{c_{in}}{\left(1+\frac{\rho}{\theta}f\cdot K_\mathrm{d}\right)}$. The term $1-\frac{\omega}{k}$ equals $\frac{\rho\cdot K_\mathrm{d}\cdot(1-f)}{\theta+\rho\cdot K_\mathrm{d}}$.

When applying the two-site model with forward and backward reactions, k_- corresponds to ω ($k_+=k_-\cdot(1-f)/f$, resulting from the kinetic sorption reaction at $t=\infty$), c^∞ to $c_0\cdot\omega/k$, and the exponent k_2/β to k used here (Nkedi-Kizza et al. 2006).

2.1.2 TSM Including First-Order Degradation/ Transformation

Assuming first-order decay/degradation in the liquid phase, the term $-\mu\cdot c(t)$ (μ in per hour) added to the right-hand side of Eq. 3 leads to the following analytical solution (most easily solved by Laplace

transformation, which can also be applied to the equations above)

$$c(t) = \frac{c_0}{2} e^{-\frac{a \cdot t}{2}} \left(e^{\frac{1}{2}\sqrt{a^2-4b} \cdot t} \left(1 - \frac{a - 2\omega}{\sqrt{a^2 - 4b}} \right) + e^{-\frac{1}{2}\sqrt{a^2-4b} \cdot t} \left(1 + \frac{a - 2\omega}{\sqrt{a^2 - 4b}} \right) \right) \quad (9)$$

with $a = \frac{\omega(\theta+\rho K_d)+\theta\mu}{\theta+\rho f K_d}$ and $b = \frac{\omega\theta\mu}{\theta+\rho f K_d}$.

2.1.3 TSM Including Irreversible Sorption

The analytical solution for the two-site model coupled to irreversible sorption, performed by the method of Laplace transformation of Eqs. 3 and 4, including the term $(ds_{irr}/dt) = k_{irr} \cdot s_2$ (k_{irr} in per hour), is the same as for the model including first-order decay (Eq. 9) but with differently defined coefficients a and b (when modeling irreversible sorption via the kinetically sorbed concentration, s_2, the additional term in the balance equation is $k_{irr} \cdot s_2$ as compared to the first-order decay term, $\mu \cdot c$):

$$a = \frac{\omega(\theta + \rho K_d)}{\theta + \rho f K_d} \text{ and } b = \frac{\omega \rho K_d (1 - f) \cdot k_{irr}}{\theta + \rho f K_d}. \quad (10)$$

The corresponding equations for s_2 and the irreversibly sorbed term are

$$s_2(t) = \frac{c_0 \cdot \omega \cdot (1-f) K_d}{\sqrt{a^2-4b}} \left\{ e^{-\frac{a \cdot t}{2}} \left(e^{\frac{1}{2}\sqrt{a^2-4b} \cdot t} - e^{-\frac{1}{2}\sqrt{a^2-4b} \cdot t} \right) \right\}$$

$$s_{irr}(t) = \frac{c_0 \cdot (\theta + \rho f K_d)}{\rho} \left\{ 1 + e^{-\frac{a \cdot t}{2}} \left(e^{-\frac{1}{2}\sqrt{a^2-4b} \cdot t} \left(\frac{a}{\sqrt{a^2-4b}} - 1 \right) - e^{\frac{1}{2}\sqrt{a^2-4b} \cdot t} \left(1 + \frac{a}{\sqrt{a^2-4b}} \right) \right) \right\}$$

In addition, we tested a simple model including one kinetic reversible sorption reaction and one irreversible reaction as described above, thus bearing four fitting parameters: k_1, k_2, k_{irr}, and c_0, and the TSM coupled with both first-order transformation in the liquid phase and irreversible sorption. Details of these models and the respective analytical solutions will be published in a forthcoming paper.

2.1.4 Second-Order Rate and Elovich Equations

We also tested the applicability of a simple second-order rate equation as used by Weber et al. (1996) to account for covalent binding: $c(t) = \frac{c_0(b_0 - c_0)}{\left(b_0 e^{k_2(b_0 - c_0)t} - c_0\right)}$, where b_0 = initial concentration of covalent binding sites and k_2 = second-order rate constant. The corresponding differential equation is $\frac{dc(t)}{dt} = k_2 \cdot c \cdot [b_0 - (c_0 - c)]$ that can, e.g., be solved by the substitution $y = c^{-1}$. The Elovich equation, $\frac{ds}{dt} = \alpha \cdot e^{-\beta s}$ (α and β are constants; Zeldovich 1934) is a widely used equation for chemisorption, nevertheless developed for gasses. This equation has been criticized because it represents various different processes and is unrealistic for $t \to \infty$ also $s \to \infty$. Nevertheless, the resulting logarithmic rate law has been successfully applied for reproducing kinetic data (Low 1960); thus, we also used it in this study. An exact solution assuming an instantaneously sorbed concentration, $s(0) = s_0$, is $s = s_0 + \ln\left(1 + t\alpha\beta \cdot e^{-\beta s_0}\right)/\beta$.

It is noted that sorption of weakly polar and nonpolar hydrophobic organic chemicals (such as trichloromethane, trichloroethylene, toluene, and phenanthrene) by soils and sediments is strongly dependent on chemical and structural properties of associated SOM (Grathwohl 1990; Huang et al. 1997). For many aquatic sediments and surface soils, Allen-King et al. (2002) stated that dominant organic materials are humic substances, and significant quantities of thermally altered carbonaceous material may be absent. Under the assumption that young SOM prevails, linear sorption behavior can be expected, whereas for thermally altered organic matter, enhanced nonlinear sorption might occur since nonpolar surfaces of potentially high specific surface area and porosity can be produced (Allen-King et al. 2002). When it is further presumed that sorption of hydrophobic organic chemicals is rather governed by a pore-filling process than sorption onto surfaces, a

Polanyi–Dubinin–Manes approach should be used (Allen-King et al. 2002; Manes 1998).

Application of a model based on diffusion will lead to a comparable righteousness of fit. Diffusion can take place into organic matter but also into matrices of expanding clay minerals for many polar organic chemicals. Pignatello (1989) for example concludes that main contributor to slow sorption is molecular diffusion. Proportionality of the sorbed concentration to $t^{1/2}$ would be an approximation of diffusion for short periods of time (e.g., Grathwohl 1998). Analytical solutions to diffusive processes coupled to sorption are given in Crank (1979) and Grathwohl (1998), such as for diffusion in a sphere: $\frac{M_t}{M_{eq_*}} = (1-\chi)\cdot\left(1-\sum_{n=1}^{\infty}\frac{6\beta(\beta+1)}{9+9\beta+q_n^2\beta^2}\exp\left(-q_n^2\frac{D_a}{a^2}t\right)\right)+\chi$, $\beta = \frac{x_{weq}}{x_{seq}} = \frac{\theta}{K_d+\frac{\varepsilon}{\rho}}$, $\tan(q_n) = \frac{3q_n}{3+\beta q_n^2}(q_n \neq 0)$, with M_t and M_{eq}=sorbed mass at time t_1 and at equilibrium, respectively, $\theta^* = 3V_w\cdot(4\pi a^3\rho)$ (ratio of volumes of the solution and (single) sphere), radius a=geometric mean of particle size distribution, x_{weq}=mass in liquid phase, x_{seq}=sorbed mass in equilibrium, and χ=fast sorbing fraction $\left(K_d^* = (1-\chi)\cdot K_d\right)$.

We also mention that batch sorption experiments might be inappropriate for investigation of kinetic processes. For example, new surfaces can develop due to the stirring of the soil samples, thus superposing the other pure sorption processes (Barrow and Shaw 1997). Therefore, the amount of shaking or stirring in a batch technique is important (e.g., Ogwada and Sparks 1986), especially when the effect of diffusion is overlaying possible quick "pure" sorption reactions. Stirring may reduce film diffusion, enhancing mass transfer to sorption sites. Still, the transfer rate ω, as used in the TSM, can be interpreted as "lumped" parameter, including possible intra-organic matter diffusion (Brusseau et al. 1991). Film diffusion might be neglected in our case due to shaking of the soil samples. Based on our data, rate limitation due to mass transfer cannot be distinguished from pure chemical kinetics. A careful interpretation of the batch sorption data is thus a prerequisite for any statements about the risk potential of the investigated substances.

The soil solution pH used of about 6–7 (Haas et al. 2010, paper in progress) is higher than the p*K*a values for AN of 4.63 (Wang et al. 2001) and NA of 3.92 (Li et al. 2001). Nevertheless, even for a pH greater than p*K*a plus two pH units, ion exchange was found to play a certain role in sorption, e.g., for aniline and α-naphthylamine (Li et al. 2001). Authors supposed enhanced protonation at the sorption surface due to a possibly depressed dielectric constant of vicinal water near clay mineral surfaces and enhanced Brønsted acidity of solvated exchangeable cations. If ion exchange has to be expected (at low pH weak organic bases can be partly protonated) besides partitioning, an additional equilibrium ion exchange model should be included, or models such as the two-site model for reversible processes including ion exchange (e.g., developed by Fábrega et al. (1998)) should be applied.

2.1.5 Adsorption Experiments

Batch sorption experiments were conducted over a time period of 3 weeks in order to investigate sorption behavior of selected aromatic amines, i.a. AN and NA, with the AM soil from a long-term field experiment (pH=6.1, 7% clay, and about 3.3% organic carbon) and Ca^{2+}-saturated montmorillonite K10 (Sigma-Aldrich; Haas et al. 2010, paper in progress). Duplicate samples (placed on a horizontal shaker with 180 movements per minute) were obtained at eight time intervals over 3 weeks, and to avoid microbial growth, 0.1 gl^{-1} Na-azide was added to the background solution (0.01 M aqueous $CaCl_2$). Initial concentrations for AN were 0.1 (AM) and 0.08 mg L^{-1} (MONTM) with solid to solution ratios of 1:20 and 0.5:4 and for NA, 11.77 mg L^{-1} (AM; MONTM) with solid to solution ratios of 1:20 and 0.1:20, respectively.

The calculated concentrations were fitted to the measured data by the nonlinear least square method with GAMS© (22.7; GAMS Development Corporation, Washington, DC, USA (2008)). Statistical analysis was performed with SPSS© (13.0; SPSS Inc., Chicago, USA (2004)). Correlation coefficients (r), root mean square errors (RMSE) of the residues, standard errors, and correlation analysis of the parameter estimates were used for comparison of the models. The diffusion equation was solved with Matlab (v. 7.0.1) applying the multidimensional nonlinear minimization module *fminsearchbnd* with bound constraints, which uses the Nelder–Mead simplex (direct search) method. This approach enables to recalculate the roots of the q_n's (see above) during the optimization procedure. We emphasize that though partly mechanistically based, the model constants will be lumped parameters due to the heterogeneity of binding sites in soils. Moreover, the solid/

solution ratios (grams/milliliter) were different for the investigated sorbent–sorbate systems (1:20 for AM, 0.5:4 for AN with MONTM, 0.1:20 for NA), thus impeding direct comparison.

2.2 Molecular Modeling

Quantum chemical calculations of bimolecular complexes of AN and NA with the set of model organic molecules acetic acid (HAc), *N*-methyl-acetamide (NMAA), imidazole (IA), and phenol (PhOH) representing functional groups in humic substances were performed both in gas and in solution. Considering pH in experiments (>6), we also took into account the deprotonized form of acetic acid (Ac^-).

All quantum chemical calculations were carried out at the DFT level of the theory by means of the computational code Turbomole (Ahlrichs et al. 1989) using the B3LYP hybrid functional (Becke 1988; Lee et al. 1988). The triple zeta valence polarization (TZVP) basis set was used in the calculations (Schäfer et al. 1994).

Full geometry optimization was performed for all complexes and corresponding individual species in the gas phase and in solution. For all systems, frequencies were also calculated in gas phase to confirm the energy minimum of the optimized structures and to obtain thermochemical quantities (interaction enthalpies, ΔH, and Gibbs free energies, ΔG). The obtained geometries in gas phase were used as a starting point for calculations in solution. The solvent effect is included in calculations via self-consistent reaction field by means of the conductor-like screening model (COSMO; Klamt and Schüürmann 1993). Water was taken as a polar solvent represented by a relative dielectric constant (ε_r =78.39) in the calculations. For a better description of the locally formed hydrogen bonds with the solvent molecules, the microsolvation model (explicit insertion of few water molecules to the model molecules) has been used. The microsolvation model together with the COSMO calculations (global solvation) was finally used in the calculations of reaction energies of the complex formation reactions. An advantage of the microsolvation model is that particular local interactions (e.g., hydrogen bonds) are described unequivocally, a characteristic which is missing in the global solvation approach. Nevertheless, the microsolvation model is size-limited, and long-range effects of a polar solvent are absent while in the global solvation approach they are included. Details on the micro-, global, and combined approaches can be found, e.g., in works by Aquino et al. (2002, 2007, 2008).

In the microsolvation approach, two water molecules were added close to the polar functional groups of all individual species and such formed complexes with water molecules were completely relaxed. As both AN and NA possess the amino ($-NH_2$) group, which can act twice as a proton donor and once as a proton acceptor (via the nitrogen atom), additional calculations with three water molecules explicitly added to the functional group were performed. The COSMO calculations were accomplished on those complexes containing water molecules as well, to get the combined micro + global solvation approach.

Reaction energies (ΔE), enthalpies (ΔH), and Gibbs free energies (ΔG) of complex formation reactions in both gas and solution (global solvation) were calculated as the difference between energies of the complex and the individual components, which can be expressed by the following general equation:

$$\mathrm{OM}\cdots x\mathrm{H_2O} + \mathrm{SM}\cdots y\mathrm{H_2O} \rightarrow \mathrm{OM}\cdots\mathrm{SM} + (\mathrm{H_2O})_{x+y} \tag{11}$$

where OM=HAc, NMAA, PhOH, IA, Ac^-, SM=AN, NA, x=0, 2, and y=0, 2, 3. If $x = y = 0$, then only gas and global solvation energies are calculated. If x=2, then y=2 or 3, and the reaction energies are calculated according to the microsolvation model. If the COSMO calculations are performed on reaction components, the energies are calculated according to the micro + global solvation model.

Harmonic vibrational frequencies and thermochemical properties such as enthalpies and Gibbs free energies were computed for the optimized structures from the gas phase calculations within the standard harmonic oscillator/rigid rotator/ideal gas approximation as available in the Turbomole program. Thermodynamic quantities were computed at room temperature (T=25°C). The enthalpy and Gibbs free energy differences for the formation of the complexes in solution were computed as the difference between the enthalpy/Gibbs free energy and the formation energy in gas phase plus the formation energy in solution according to

$$\Delta H_s = \Delta H_g - \Delta E_g + \Delta E_s, \quad \text{and} \tag{12}$$

$$\Delta G_s = \Delta G_g - \Delta E_g + \Delta E_s \tag{13}$$

where subscripts "g" and "s" represent gas and solution phase, respectively.

Note that in the reaction scheme (Eq. 11), four/five water molecules on the side of reactants are considered as tetramer or pentamer clusters and not as four/five individual molecules. Reaction energies calculated from the microsolvation approach will be denoted by the subscript "ms" and from the micro + global solvation approach by the subscript "gms," respectively.

Calculated interaction energies are not corrected for basis set superposition error (BSSE) since it was already shown that for basis sets increased with polarization functions, the BSSE is reduced substantially for hydrogen-bonded complexes (Aquino et al. 2002, 2008; Tunega et al. 2000).

3 Results and Discussion

3.1 Kinetic Sorption Concepts

In Table 1 the analytically solved models (of the method section) are listed. Only results of fitting two data sets of NA and AN sorption onto AM and montmorillonite, obtained with the two-site model including irreversible sorption (model (c), Fig. 1, Table 2), are discussed. Some general conclusions follow at the end of this section.

Models (b) and (c) fit all sorption systems well, with the same correlation coefficients, RMSE values, and confidence intervals and thus are statistically not distinguishable. Interpretation of the results is complicated due to the simplified model assumptions generating lumped parameters and the high number of fitting parameters (three to four) as compared to the number of data points used (16).

Model (c) results in higher irreversible reaction rates for the soil as compared to MONTM for AN and NA ($k_{irr,AM} > k_{irr,,MONTM}$) and higher fractions of equilibrium sorption places and K_d values for AN sorbed to AM ($f_{AM} > f_{MONTM}, K_{d,AM} > K_{d,MONTM}$), whereas the opposite trend is observed for NA (Table 2, the latter sequence with regard to K_d holds for all models (a) to (c)). Regarding the transfer rate, $\omega_{AM} < \omega_{MONTM}$ for all systems and model concepts (thus, equilibrium is attained more quickly in case of MONTM). The higher rates for MONTM might be explained by easier accessible, planar adsorption sites of the mineral. For the model accounting for first-order decay (model (b)), the factor μ is approximately one to two orders less for montmorillonite as compared to the respective values for AM, with comparable (AN and NA) values for f and K_d regarding model (c). For all systems, the simulated initial concentration in liquid phase (c_0) fits much better to the measured equilibrium concentrations for MONTM as compared to AM, probably indicating that for AM, additional equilibrium reactions would have to be accounted for to simulate a steeper gradient at the beginning of the experiment.

We emphasize that without additional measurements (e.g., regarding degradation), the most appropriate model cannot be unambiguously selected. A model accounting for both irreversible sorption and degradation/transformation, nevertheless, seems to be the most reasonable concept since both processes can be expected to occur for the investigated sorbates (at least for AM). For this model, the rates of decay and irreversible sorption (which are highly correlated parameters) cannot be fitted independently. Solely when, e.g., the decay rate could be measured in an independent experiment, such a concept would be more reasonable. It is noted here that the term for transformation could also be interpreted as linear irreversible reaction directly from the liquid phase, as parallel reaction to the sorption processes.

The magnitude of overall sorption is higher for NA than for AN, which could be explained by the higher hydrophobicity of NA (log $K_{ow,NA}$=2.25, log $K_{ow,AN}$= 0.92), being in line with other studies (e.g., Karickhoff (1980); Pignatello (1989); Li et al. (2001)). For MONTM higher transfer rates are found for NA as compared to AN. Regarding irreversible sorption, a maximum of irreversible binding sites would be more realistic (though not feasible in our case since the amount of fitting parameters would be too high then), e.g., by including a Langmuir-type equation instead of the linear term, or by exchanging a linear irreversible reaction in model (c) by a second-order rate equation

Table 1 Models solved analytically for fitting kinetic sorption

Model	Fitting Parameter
(a) Two-site model (TSM)	K_d, f, ω
(b) TSM with first-order decay/transformation	K_d, f, ω, μ
(c) TSM including irreversible sorption	K_d, f, ω, k_{irr}

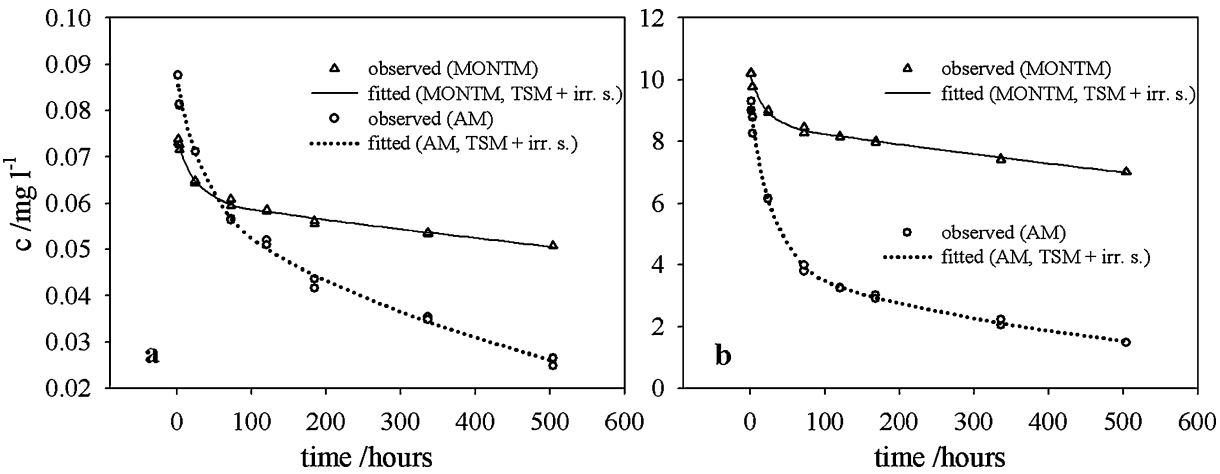

Fig. 1 Observed versus fitted results of aniline (**a**) and 1-naphthylamine (**b**) on AM-treated soil and montmorillonite

as used by Weber et al. (1996), e.g., $\frac{ds_{irr}}{dt} = k_{irr} \cdot s_2 \cdot \left[b_0 - (s_{2,0} - s_2)\right]$.

The simple two-site model is insufficient to match the measured solute concentrations. Diffusive processes will contribute to the investigated behavior with regard to the AM soil, but probably also to montmorillonite. Despite stirring during the batch experiments, diffusion into organic matter but also montmorillonite interlayer spaces will most likely contribute to the observed concentration distribution over time, at least for the smaller molecule aniline, and presumably in combination with various sorption and degradation processes (since no clear, linear dependency of the concentration and $t^{1/2}$ as indicator for diffusive processes can be found). Most likely, two successive diffusion processes contribute to the overall observed behavior of all substances (fast diffusion at the beginning, followed by a slow one after approx. 1 to 3 days). Inverse parameter estimation by applying the diffusion equation leads to comparable fit results as models (b) and (c), nevertheless with solely three fitting parameters, supposed the mean particle radius, a, is known. Results for MONTM (with a=7.8 μm) and AN (r=0.994, RMSE=8.28×10^{-4}) are D=4.05×10^{-10} cm^2 h^{-1}, K_d=4.03 ml g^{-1} (K_d^*=3.7), χ=0.0744; and for NA (r=0.991, RMSE=0.136): D=3.15×10^{-10} cm^2 h^{-1}, K_d=137.5 ml g^{-1} (K_d^*=94.7), χ=0.3115. Thus, the K_d values are in the same order as for the other kinetic sorption concepts, and also, the fractions of equilibrium sorption, χ, are comparable to the fractions f of the kinetic sorption concepts.

The second-order rate equation as used by Weber et al. (1996), without additional terms added, does not lead to improved fits, with correlation coefficients below the ones of all other models listed above. Applying an exact solution of the Elovich equation, we get good curve fitting results, especially for AN/MONTM (r=0.999). Anyhow, the standard errors of the parameter estimates for NA are much too high to

Table 2 Fitted parameters (standard errors in parentheses) for AN and NA—two-site model coupled with a term for irreversible sorption (model (c))

Solute/sorbent	f	K_d	ω	k_{irr}	c_0[a]	RMSE	r
AN/AM	0.192 (0.037)	18.3 (3.6)	0.016 (0.007)	4.86×10^{-3} (1.35×10^{-3})	0.0862	2.08×10^{-3}	0.995
AN/MONTM	0.146 (0.024)	2.3 (0.1)	0.034 (0.006)	1.97×10^{-3} (0.27×10^{-3})	0.0739	5.92×10^{-4}	0.997
NA/AM	0.122 (0.008)	45.6 (3.0)	0.013 (0.002)	3.30×10^{-3} (0.41×10^{-3})	9.2	0.110	0.999
NA/MONTM	0.396 (0.030)	79.2 (4.0)	0.042 (0.011)	2.46×10^{-3} (0.42×10^{-3})	10.2	0.112	0.994

[a] Calculated equilibrium concentration at t=0 after instantaneous partitioning; the measured input concentration $c_{in,AN}$=0.10/0.08 mg l^{-1} for AM and MONTM, respectively, and $c_{in,NA}$=11.8 mg l^{-1}

allow for interpretation. In principle, the high values for α, interpreted as initial rate of adsorption, would indicate that quasi-equilibrium processes prevail at the beginning of the experiment. Similar goodness of fit can be obtained with an analytical Elovich-type equation as cited in Ho (2006) (this equation resembles the analytical solution above, but only the multiplication sign being exchanged by a plus sign in the second term (see section "Second-Order Rate and Elovich Equations")).

With regard to AN adsorption on montmorillonite, intercalation and polymerization can also be expected. For example, such processes were suggested for AN at least above a critical concentration adsorbing on montmorillonite saturated with Cu^{2+} or Na^{+} (Ilic et al. 2000; Nascimento et al. 2004). Thus, a polymerization process will also most likely occur with regard to Ca-montmorillonite at higher concentrations. With regard to NA, Ainsworth et al. (1991) suggested that in the presence of Fe^{3+}, sorption of NA onto smectite clays was followed by a transformation reaction between the formed radical cation–clay complex and the neutral NA molecule at ditrigonal cavities in the tetrahedral layers. Thus, a term like $\mu_s cs_2$ (times some fraction of "activation sorption sites") could be added to the TSM. No explicit solution can be found for this model, whereas Matlab (v. 7.0.1) simulations, with this second-order reaction term coupled to the simple TSM, gave good agreement with experimental NA/MONTM data (using multidimensional unconstrained minimization, applying a simplex search method): K_d=77.7, ω=0.0450, f=0.402, $\mu_s=3.29\times10^{-4}$, c_0=10.2, R^2=0.995. These values for K_d, f, and ω are similar to the results calculated with models (b) and (c).

The different sorption behavior of AN and NA was also discussed by Li et al. (2001) and Lee et al. (1997). The authors observed that both, degree of nonlinearity and magnitude of sorption, were less for AN relative to NA. For given amine–soil combination, sorption generally decreased with increasing soil solution pH as amine speciation shifted to the neutral species. At given solution pH, sorption increased with increasing SOM and CEC. Conducting competitive sorption experiments, AN sorption was found to be influenced by NA, whereas NA was not strongly affected by sorption of AN when both solutes exist as cations. This demonstrated the stronger selectivity of cation exchange sites for NA than for AN (and was in line with the observation by, e.g., Zachara et al. (1987) that selectivity increases with the number of fused rings).

3.2 Molecular Modeling

The stability of the complexes of NA and AN in gas and liquid phases has been computed on the basis of calculated reaction energies of model reactions (Eq. 11). The calculated thermodynamic quantities are collected in Tables 3 (gas phase and global

Table 3 B3LYP/TZVP calculated formation energies, enthalpies, and Gibbs free energies (in kilocalories per mole) of different complexes in gas and in solution (global solvation—COSMO approach)

Complex formation reaction	Gas			Solution		
	ΔE_g	ΔH_g	ΔG_g	ΔE_s	ΔH_s	ΔG_s
Aniline						
HAc + AN → HAc···AN	−9.1	−7.5	1.7	−4.8	−3.2	6.0
NMAA + AN → NMAA···AN	−7.6	−5.9	3.6	−1.1	0.6	10.1
IA + AN → IA···AN	−5.2	−3.8	2.9	−1.5	−0.2	6.6
PhOH + AN → PhOH···AN	−6.0	−5.0	5.0	−4.0	−3.0	7.0
Ac^- + AN → $[HAc\cdots AN]^-$	−20.4	−19.5	−11.0	−0.6	0.3	8.9
1-Naphthylamine						
HAc + NA → HAc···NA	−9.0	−7.4	1.8	−4.3	−2.7	6.5
NMAA + NA → NMAA···NA	−7.6	−5.9	3.4	−1.0	0.7	10.0
IA + NA → IA···NA	−4.9	−3.5	3.8	−1.4	0.0	7.3
PhOH + NA → PhOH···NA	−5.7	−4.1	3.9	−3.7	−2.1	5.9
Ac^- + NA → $[Ac\cdots NA]^-$	−24.0	−23.2	−14.8	−0.7	0.09	8.5

solvation) and 4 (microsolvation and micro + global solvation), respectively. Figures 2, 3, and 4 display the gas phase optimized structures of all complexes. In all complexes investigated, hydrogen bonding dominates as the main formation mechanism. The optimized hydrogen bond lengths are depicted in each structure in Figs. 2, 3, and 4 for gas and solution.

Since AN and NA have the same functional amino group, they originate the same type of complexes with the selected set of molecules as can be seen from Figs. 2, 3, and 4. The differences in the hydrogen bonds formed of AN and NA are very small. The amino group can act in hydrogen bonds either as a proton donor via two H atoms or as a proton acceptor via an electron ion pair localized on the nitrogen atom. The hydrogen bonds formed are of relatively weak or moderate strength. The strongest hydrogen bond is observed for the complex with the acetic acid where the $–NH_2$ group is a proton acceptor of the hydrogen atom from the carboxyl group (Figs. 2b and 3b). The second weaker hydrogen bond is formed between one of two hydrogen atoms of the $–NH_2$ group and the carbonyl oxygen atom of the –COOH group. The solvent effect increases the strength of the hydrogen bonds of the HAc since both hydrogen bonds become shorter under this effect. Acetamide also forms complexes with two hydrogen bonds (Figs. 2a and 3a). Both hydrogen bonds are relatively weak with lengths of 2.1–2.2 Å in gas phase. One of these hydrogen bonds is formed between the carbonyl group (proton acceptor) and the $–NH_2$ group of AN/NA. The second hydrogen bond is formed between one hydrogen atom of the $–NH_2$ group of the NMAA and the nitrogen atom of the AN/NA molecule. Opposite to HAc, both hydrogen bonds of NMAA become weaker under the solvent effect as document longer hydrogen bonds depicted in Figs. 2a and 3a, respectively. For imidazole the $–NH_2$ group of AN/NA donates a proton to the nitrogen atom in the IA aromatic ring forming a relatively weak hydrogen bond (>2.1 Å). The imidazole molecule can also form a hydrogen bond via the –NH group of the aromatic ring.

Table 4 B3LYP/TZVP calculated formation energies, enthalpies, and Gibbs free energies (in kilocalories per mole) of different complexes using microsolvation and micro + global solvation approach

Complex formation reaction	Microsolvation			Micro + global solv.		
	ΔE_{ms}	ΔH_{ms}	ΔG_{ms}	ΔE_{mgs}	ΔH_{mgs}	ΔG_{mgs}
Aniline						
$HAc\cdots 2H_2O + AN\cdots 2H_2O \rightarrow HAc\cdots AN + (H_2O)_4$	−0.31	−0.18	−0.33	−2.93	−2.80	−2.95
$NMAA\cdots 2H_2O + AN\cdots 2H_2O \rightarrow NMAA\cdots AN + (H_2O)_4$	−0.65	−0.70	−1.09	−1.07	−1.11	−1.50
$IA\cdots 2H_2O + AN\cdots 2H_2O \rightarrow IA\cdots AN + (H_2O)_4$	−5.03	−5.01	−2.34	−2.62	−2.60	0.07
$PhOH\cdots 2H_2O + AN\cdots 2H_2O \rightarrow PhOH\cdots AN + (H_2O)_5$	−3.20	−3.88	−1.90	−6.21	−6.88	−4.91
$HAc\cdots 2H_2O + AN\cdots 2H_2O \rightarrow HAc\cdots AN + (H_2O)_5$	−0.07	0.03	−0.70	−1.71	−1.61	−2.34
$NMAA\cdots 2H_2O + AN\cdots 2H_2O \rightarrow NMAA\cdots AN + (H_2O)_5$	−0.41	−0.49	−1.45	0.16	0.07	−0.89
$IA\cdots 2H_2O + AN\cdots 2H_2O \rightarrow IA\cdots AN + (H_2O)_5$	−4.79	-4.80	−2.71	−1.40	−1.41	0.68
$PhOH\cdots 2H_2O + AN\cdots 2H_2O \rightarrow PhOH\cdots AN + (H_2O)_5$	−2.96	−3.66	−2.27	−4.99	−5.69	−4.30
$[Ac\cdots 2H_2O]^- + AN\cdots 2H_2O \rightarrow [AN\cdots Ac]^- + (H_2O)_5$	2.40	1.55	1.14	3.67	2.82	2.41
1-Naphthylamine						
$HAc\cdots 2H_2O + NA\cdots 2H_2O \rightarrow HAc\cdots AN + (H_2O)_4$	−0.09	0.07	−0.47	−2.55	−2.39	−2.93
$NMAA\cdots 2H_2O + NA\cdots 2H_2O \rightarrow NMAA\cdots AN + (H_2O)_4$	−0.58	−0.61	−1.58	−1.14	−1.17	−2.14
$IA\cdots 2H_2O + NA\cdots 2H_2O \rightarrow A\cdots NA + (H_2O)_4$	−4.64	−4.57	−1.74	−2.60	−2.53	0.29
$PhOH\cdots 2H_2O + NA\cdots 2H_2O \rightarrow PhOH\cdots NA + (H_2O)_4$	−2.91	−2.89	−3.25	−6.06	−6.04	−6.39
$HAc\cdots 2H_2O + NA\cdots 2H_2O \rightarrow HAc\cdots AN + (H_2O)_5$	−0.07	0.05	−0.89	−1.62	−1.49	−2.43
$NMAA\cdots 2H_2O + NA\cdots 2H_2O \rightarrow NMAA\cdots AN + (H_2O)_5$	−0.57	−0.62	−2.00	−1.43	−1.48	−2.85
$IA\cdots 2H_2O + NA\cdots 2H_2O \rightarrow A\cdots NA + (H_2O)_5$	−4.62	−4.59	−2.16	−1.67	−1.63	0.79
$PhOH\cdots 2H_2O + NA\cdots 2H_2O \rightarrow PhOH\cdots NA + (H_2O)_5$	−2.90	−2.32	−3.67	−5.13	−4.55	−5.89
$[Ac\cdots 2H_2O]^- + NA\cdots 2H_2O \rightarrow [NA\cdots Ac]^- + (H_2O)_5$	−1.28	−2.19	−2.99	3.02	2.11	1.31

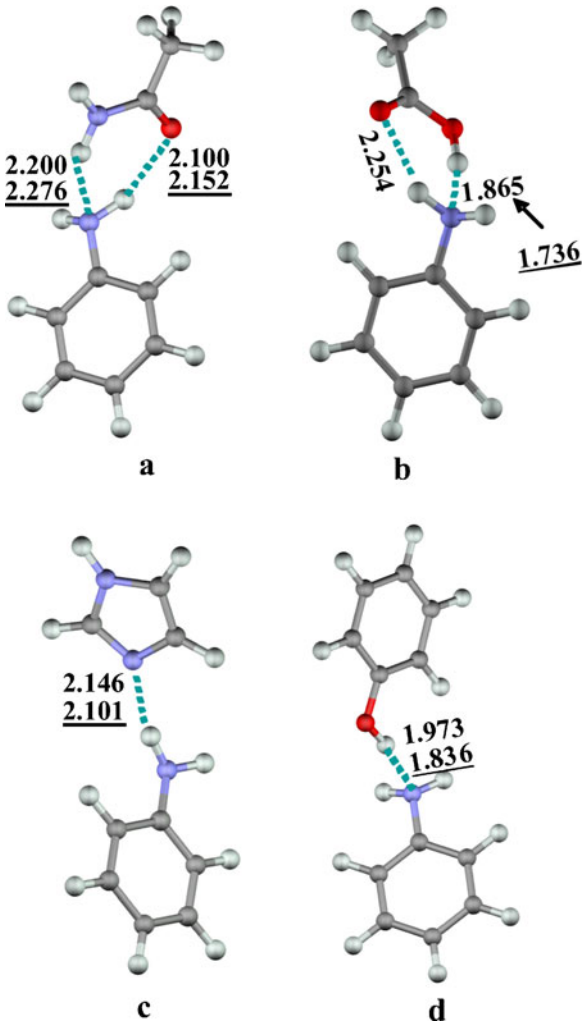

Fig. 2 Structure and hydrogen bond distances (in Ångstrom) in gas phase and in solution (*underlined values*) of the complexes of aniline with **a** acetamide, **b** acetic acid, **c** imidazole, and **d** phenol

Inspection of this configuration shows that such complex with AN/NA is weaker than those displayed in Figs. 2c and 3c, respectively. Thus, only more stable complexes of imidazole are discussed in this work. The solvent effect evokes shortening of the hydrogen bond in AN/NA···IA complexes. The complex of AN/NA with phenol is formed via one hydrogen bond with the length of about 1.9Å (Figs. 2d and 3d). In this hydrogen bond, the -OH group is a proton donor to the $–NH_2$ group. The solvent effect leads to significant shortening of the hydrogen bond, i.e., stabilization of the AN/NA···PhOH complex in solvent.

To include the effect of pH>6, where acetic acid is deprotonated, the complexes of acetate anion with the neutral AN/NA molecules have been investigated as well (Fig. 4a, b). A cyclic complex with two nonequivalent hydrogen bonds is formed where both carbonyl oxygen atoms of the $–COO^-$ group are proton acceptors. One hydrogen bond is relatively strong (~1.8Å) while the second one is weak, having O···H distance of ~2.4Å. The solvent effect results in significant weakening of the strong hydrogen bond in the complexes of acetate anion as is evident from the elongation of the O···H distance (see Fig. 4). Moreover, the weak hydrogen bond in the Ac^-···AN complex disappears, and in the case of the Ac^-···NA complex, the hydrogen bond becomes very weak under the solvent effect.

Calculated formation energies, enthalpies, and Gibbs free energies for reactions without microsolvation (no explicit insertion of H_2O molecules $x = y = 0$ in Eq. 11) are collected in Table 3. Comparison of the formation energies of AN and NA also confirmed that both molecules form similar complexes with the set of selected species. The energetically strongest complex is formed with HAc (ΔE= −9.1 kcal mol^{-1} for AN in gas phase) that matches to the formation of two hydrogen bonds from which one is relatively strong. Generally, the order of the stability of neutral complexes corresponds to the number and character of the formed hydrogen bonds as discussed above. The second most stable complex is formed with NMAA and also two hydrogen bonds exist. The weakest complex is formed with imidazole, for which only a weak hydrogen bond is created. The acetate anion forms energetically very stable complexes with AN/NA as indicated by the formation energy ΔE of about −20 kcal mol^{-1} for AN. While thermal corrections to ΔE for the association reaction are relatively small and ΔH is only slightly smaller than ΔE, the entropic contributions, $T\Delta S$, are large. For example, $T\Delta S$ for the complex HAc···NA is −9.2 kcal mol^{-1}. This outsized entropy loss is characteristic for associative reactions like $A + B \rightarrow C$, due to the transformation of rotational and translational degrees of freedom in the isolated molecules to vibrational degrees of freedom in the complex. Generally, a large value of $T\Delta S$ means that only strongly bound complexes can be stable in the gas phase at room temperature. Calculated ΔG_g values for the gas phase reactions (Table 3) document

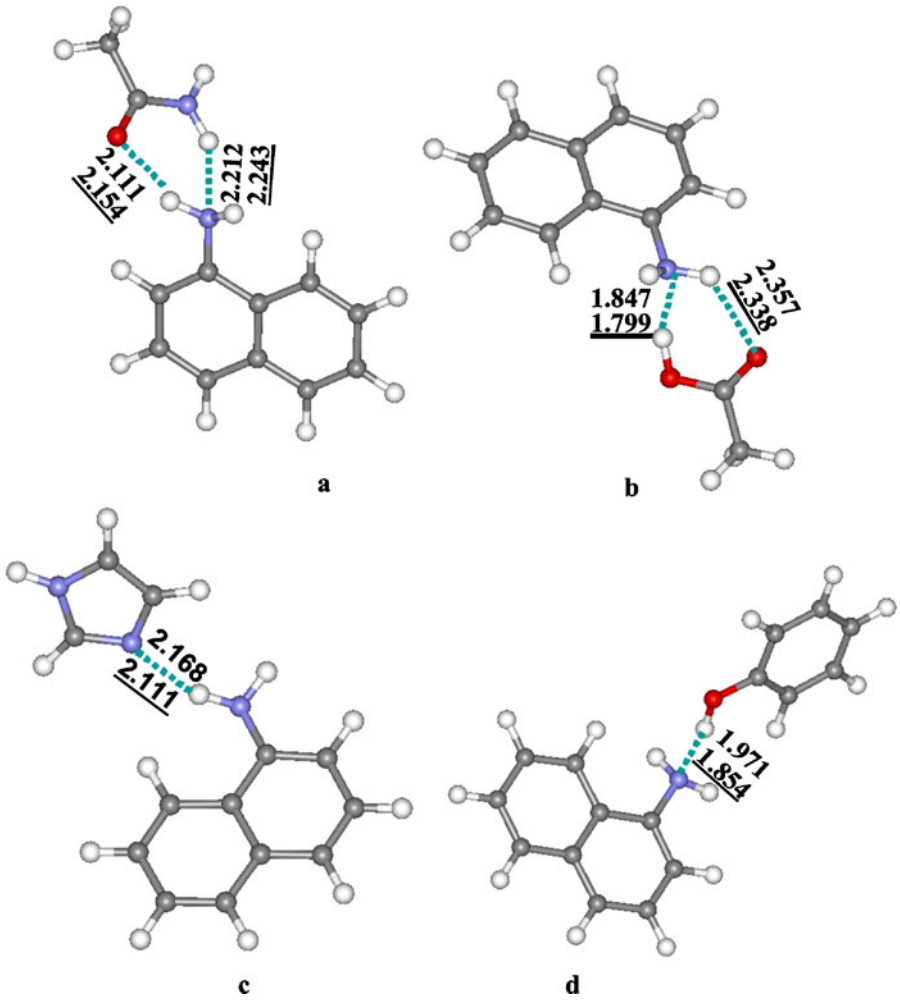

Fig. 3 Structure and hydrogen bond distances (in Ångstrom) in gas phase and in solution (*underlined values*) for complexes of 1-naphthylamine with **a** acetamide, **b** acetic acid, **c** imidazole, and **d** phenol

that complexes formed from neutral reactants are thermodynamically unstable at room temperature including the strongest HAc···AN/NA complexes. The charged Ac^{-}···AN/NA complexes have ΔG_g values clearly negative what confirms their thermodynamic stability in the gas phase.

The association reactions in the solution are strongly affected by the solvent effect. The complexation energies in solution, ΔE_s, obtained from the global (COSMO) approach for the AN/NA complexes decrease significantly when compared to the results obtained for gas phase (Table 3). This strong reduction is due to the loss of solvent accessibility to the polar surface area of the complexes in comparison to the isolated reactants whose polar functional groups are available for interaction with the polar solvent. This effect was investigated in detail for various hydrogen-bonded complexes in our previous work (Aquino et al. 2002) and also shown in our paper on complexes of 2,4-dichloro-phenoxy-acetic acid (2,4-D; Aquino et al. 2007). Thermal effects and entropy changes in solution were taken from the gas phase calculations according to Eqs. 12 and 13. The results obtained indicate that none of the AN/NA complexes formed from neutral reactants would be stable in the polar solvent considering the clearly positive values for ΔG_s (Table 3). The solvent effect is even stronger in case of charged reactants or products. An enormous decrease of the reaction energies is observed for the complexes formed from the acetate anion. In case of the Ac^{-}···AN/NA complexes, ΔG_s is positive which indicates that such complexes would be unstable in solution. The observed differences in reaction energies for neutral and charged reactants (i.e., acetic acid, acetate) show that solution's pH will play an important role in the

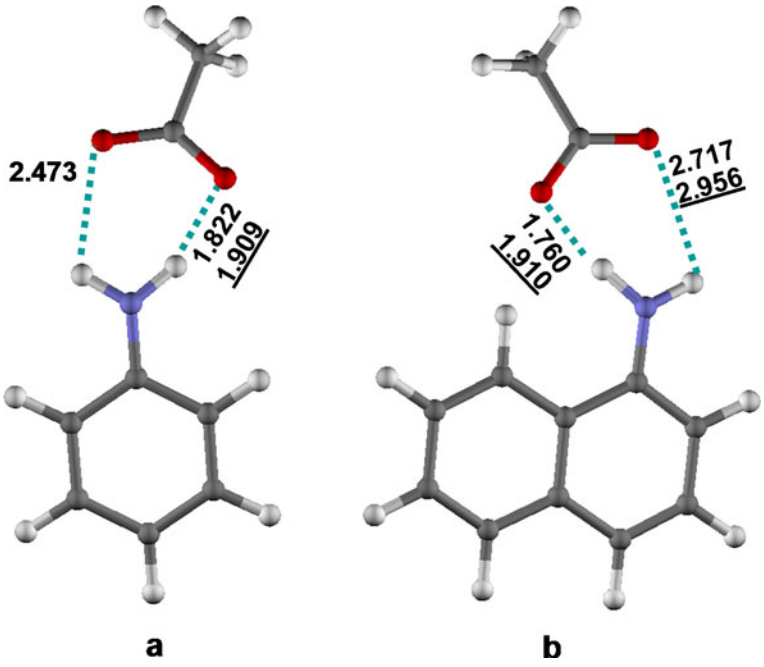

Fig. 4 Structure and hydrogen bond distances (in Ångstrom) in gas phase and in solution (*underlined values*) for complexes of **a** aniline and **b** 1-naphthylamine with acetate

formation of complexes since it will control the prevailing form of reactants.

However, conclusions based on the associative reaction scheme cannot be fully correct. Using only a polarizable continuum model for the solvation effect means that specific interactions like hydrogen bonds will not be well described and, moreover, the type of association reaction A + B → C is not optimal for the description of the formation of complexes in solvent. Such reactions are of exchange reaction type. This problem could be overcome if reactants are explicitly solvated, thus specifically interacting with polar solvent molecules in the form of hydrogen bonds (microsolvation approach, x=2, y=2,3, Eq. 11. This model was applied in our study of the 2,4-D complexes (Aquino et al. 2007) and most recently for acrylic acid complexes (Aquino et al. 2008). The results of the combined micro + global solvation approach can be considered as the most complete description of the complex formation reactions in solution. The complexation energies for AN/NA molecules resulting from such approach are shown in Table 4.

It is clear from the values of the reaction enthalpies and Gibbs free energies that the entropy loss is noticeably smaller now as compared to the complex formation of the association reactions (Table 3). Furthermore, the comparison of the Gibbs free energies from micro and micro + global solvation approaches shows that also the global solvent effect obtained from the COSMO approach is smaller than in the case of association reactions if neutral reactants are considered. The global solvent effect is still large in case of reaction between charged reactants when the neutral HAc···AN/NA complexes are formed. The exchange reaction approach using explicit solvation yields different order of stability of the complexes compared to the associative reaction approach. It seems from the Gibbs free energies of neutral reactants in Table 4 that except the complex with imidazole, which is not stable with micro + global solvation approach, all other complexes can be stable according to both microsolvation and micro + global solvation approaches. Results obtained either with two or three water molecules used in the explicit solvation of the neutral reactants are very similar (see Table 4). According to the calculated Gibbs free energies, the complex of phenol is the most stable complex, which is different from the results obtained on the basis of the association reaction scheme. However, the discussion of the stability of the complexes has to be conducted carefully since ΔG calculated based on exchange reaction scheme are not so far from zero. Care has to be taken in case of the

charged Ac^{-}···AN/NA complexes as the micro + global solvation approach gave only slightly positive Gibbs free energies. However, it is important to emphasize that the significance of reaction schemes is dependent on the concentration of the reactants in solution that is strongly pH related.

The free energies of formation for the test set collected in Table 4 (micro + global solvation) show a slight but significant preference for the interactions involving NA as can be seen, e.g., in the cases of interactions with NMAA, PhOH, and Ac^{-}. As stated above, these cases should represent interaction in HS. Experimentally (see Table 2), a stronger preference of NA adsorption is observed as compared to AN, which could be explained by different hydrophobicities of these two compounds. Such more detailed analysis goes beyond the scope of the present work since a significantly more extended molecular model would be required and explicit molecular dynamics and/or Monte Carlo calculations need to be performed.

4 Conclusion

Results by applying semi-mechanistically based kinetic sorption concepts show that for the investigated sorbate–sorbent systems consisting of aromatic amines (AN, NA) and two sorbents (arable soil (AM), MONTM), consideration of either both time-dependent sorption processes and transformation and/or irreversible sorption processes, or explicitly accounting for diffusion into the sorbent coupled to fast and slow sorption mechanisms are necessary in order to correctly predict the fate and risk potential of these substances. By fitting the respective kinetic model parameters, the chosen models could well reproduce the long-time behavior of the sorbates. In general, the magnitude of overall sorption is higher for NA than for AN, reflecting the higher hydrophobicity of NA. The transfer rate is higher for MONTM for all systems and model concepts, thus equilibrium is attained more quickly as compared to AM as expected. The simple two-site model is insufficient to reproduce the measured concentrations over time. An analytical solution to the diffusion equation coupled to instantaneous sorption led to good results with the advantage of reduced amount of fitting parameters (three as compared to four).

Quantum chemical calculations on free energies of complex formation have been performed on hydrogen-bonded interactions of NA and AN with selected functional groups occurring in HS. The respective data show a slight preference of NA sorption in comparison to AN. On the other hand, the experimental data on AM show a pronounced preference for NA sorption. There is a wide range of possibilities for additional factors relevant for the different adsorption behavior of NA versus AN, where hydrophobic interaction is one of them, but pH dependence leading to protonation/deprotonation is another one. The complexity of these additional possibilities obviously requires more experimental investigations and concomitant enhancement of the molecular models.

Acknowledgments This work was supported by the Austrian Sciences Fund (project P17967-N11) and by the German Research Foundation, priority program SPP 1315, Project GE 1676/1-1. The calculations were performed in part on the Schrödinger III cluster of the University of Vienna.

References

Ahlrichs, R., Bär, M., Häser, M., Horn, H., & Kölmel, C. (1989). Electronic structure calculations on workstation computers: The program system Turbomole. *Chemical Physics Letters, 162*, 165–169.

Ainsworth, C. C., McVeety, B. D., Smith, S. C., & Zachara, J. M. (1991). Transformation of 1-aminonaphthalene at the surface of smectite clays. *Clays and Clay Minerals, 39*, 416–427.

Allen-King, R. M., Grathwohl, P., & Ball, W. P. (2002). New modeling paradigms for the sorption of hydrophobic organic chemicals to heterogeneous carbonaceous matter in soils, sediments, and rocks. *Advances in Water Resources, 25*, 985–1016.

Aquino, A. J. A., Tunega, D., Haberhauer, G., Gerzabek, M. H., & Lischka, H. (2002). Solvent effects on hydrogen bonds—a theoretical study. *The Journal of Physical Chemistry. A, 106*, 1862–1871.

Aquino, A. J. A., Tunega, D., Haberhauer, G., Gerzabek, M. H., & Lischka, H. (2007). Interaction of the 2,4-dichlorophenoxy-acetic acid herbicide with soil organic matter moieties—a theoretical study. *European Journal of Soil Science, 58*, 889–899.

Aquino, A. J. A., Tunega, D., Pašalić, H., Haberhauer, G., Gerzabek, M. H., & Lischka, H. (2008). The thermodynamic stability of hydrogen-bonded and cation-bridged complexes of humic acid models—a theoretical study. *Chemical Physics, 349*, 69–76.

Barrow, N. J., & Shaw, T. C. (1997). Effects on solution: soil ratio and vigour of shaking on the rate of phosphate adsorption by soil. *Soil Science, 119*, 167–177.

Becke, A. D. (1988). Density-functional exchange-energy approximation with correct asymptotic behavior. *Physical Review A, 38*, 3098–3100.

Brusseau, M. L., Jessup, R. E., & Rao, S. C. (1991). Nonequilibrium sorption of organic chemicals: elucidation of rate-limiting processes. *Environmental Science & Technology, 25*, 134–142.

Crank, J. (1979). *The mathematics of diffusion* (2nd ed.). Oxford: Oxford University Press.

Delle Site, A. (2001). Factors affecting sorption of organic compounds in natural sorbent/water systems and sorption coefficients for selected pollutants. A review. *Journal of Physical and Chemical Reference Data, 30*, 187–439.

Dixon, J. B., & Schulze, D. G. (2002). *Soil mineralogy with environmental applications*. Madison: Soil Science Society of America.

Fábrega, J. R., Jafvert, C. T., Li, H., & Lee, L. S. (1998). Modeling short-term soil-water distribution of aromatic amines. *Environmental Science & Technology, 32*, 2788–2794.

Gevao, B., Semple, K. T., & Jones, K. C. (2000). Bound pesticide residues in soils: A review. *Environmental Pollution, 108*, 3–14.

Ghabbour, E. A., & Davis, G. (2000). *Humic substances—versatile components of plants, soils and water*. Cambridge: Royal Society of Chemistry.

Grathwohl, P. (1990). Influence of organic matter from soils and sediments from various origins on the sorption of some chlorinated aliphatic hydrocarbons: Implications on K_{OC} correlations. *Environmental Science & Technology, 24*, 1687–1693.

Grathwohl, P. (1998). *Diffusion in natural porous media: contaminant transport, sorption/desorption and dissolution kinetics*. Norwell: Kluwer.

Ho, Y. S. (2006). Review of second-order models for adsorption systems. *Journal of Hazardous Materials, 136* (3), 681–689.

Huang, W., Young, T. M., Schlautman, M. A., Yu, H., & Weber, W. J., Jr. (1997). A distributed reactivity model for sorption by soils and sediments. 9. General isotherm nonlinearity and applicability of the dual reactive domain model. *Environmental Science & Technology, 31*, 1703–1710.

Ilic, M., Koglin, E., Pohlmeier, A., Narres, H. D., & Schwuger, M. J. (2000). Adsorption and polymerization of aniline on Cu(II)-montmorillonite: Vibrational spectroscopy and ab initio calculation. *Langmuir, 16*, 8946–8951.

Karickhoff, S. W. (1980). Sorption kinetics of hydrophobic pollutants in natural sediments. Chapter 11. In R. A. Baker (Ed.), *Contaminants and sediments. Analysis, chemistry, biology* (Vol. 2, pp. 193–205). Ann Arbor, Michigan: Ann Arbor Science.

Karickhoff, S. W., & Morris, K. R. (1985). Sorption dynamics of hydrophobic pollutants in sediment suspensions. *Environmental Toxicology and Chemistry, 4*, 469–479.

Kile, D. E., Wershaw, R. L., & Chiou, C. T. (1999). Correlation of soil and sediment organic matter polarity to aqueous sorption of nonionic compounds. *Environmental Science & Technology, 33*, 2053–2056.

Klamt, A., & Schüürmann, G. (1993). COSMO: a new approach to dielectric screening in solvents with explicit expressions for the screening energy and its gradient. *Journal of the Chemical Society—Perkin Transactions, II*, 799–805.

Lee, C., Yang, W., & Parr, R. G. (1988). Development of the Colle–Salvetti correlation-energy formula into a functional of the electron density. *Physical Review B, 37*, 785–789.

Lee, L. S., Nyman, A. K., Li, H., Nyman, M. C., & Jafvert, C. (1997). Initial sorption of aromatic amines to surface soils. *Environmental Toxicology and Chemistry, 16*, 1575–1582.

Li, H., Lee, L. S., Fabrega, J. R., & Jafvert, C. T. (2001). Role of pH in partitioning and cation exchange of aromatic amines on water-saturated soils. *Chemosphere, 44*, 627–635.

Low, M. J. D. (1960). Kinetics of chemisorption of gases on solids. *Chemical Reviews, 60*, 267–312.

Manes, M. (1998). Activated carbon adsorption fundamentals. In R. Meyers (Ed.), *Encyclopedia of environmental analysis and remediation* (pp. 26–67). New York: Wiley.

Nascimento, G. M., Constantino, V. R. L., Landers, R., & Temperini, M. L. A. (2004). Aniline polymerization into montmorillonite clay: a spectroscopic investigation of the intercalated conducting polymer. *Macromolecules, 37*, 9373–9385.

Nkedi-Kizza, P., Shinde, D., Savabi, M. R., Ouyang, Y., & Nieves, L. (2006). Sorption kinetics and equilibria of organic pesticides in carbonatic soils from South Florida. *Journal of Environmental Quality, 35*, 268–276.

Ogwada, R. A., & Sparks, D. L. (1986). Kinetics of ion exchange on clay minerals and soils: II. Elucidation of rate-limiting steps. *Soil Science Society of America Journal, 50*, 1162–1164.

Parker, A., & Rae, J. E. (1998). *Environmental interactions of clays*. Berlin: Springer.

Parris, G. E. (1980). Covalent binding of aromatic amines to humates. 1. Reactions with carbonyls and quinones. *Environmental Science & Technology, 14*, 1099–1106.

Pignatello, J. J. (1989). Sorption dynamics of organic compounds in soils and sediments. In B. L. Sawhney & K. Brown (Eds.), *Reactions and movements of organic chemicals in soils* (2nd ed., pp. 45–80). (SSSA Special Publication 22) SSSA: Madison.

Pignatello, J. J. (2000). The measurement and interpretation of sorption and desorption rates for organic compounds in soil media. *Advances in Agronomy, 69*, 1–73.

Schäfer, A., Huber, C., & Ahlrichs, R. (1994). Fully optimized contracted gaussian basis sets of triple zeta valence quality for atoms Li to Kr. *The Journal of Chemical Physics, 100*, 5829–5835.

Schwarzenbach, R. P., & Westall, J. (1981). Transport of nonpolar organic compounds from subsurface water to groundwater, Laboratory sorption studies. *Environmental Science & Technology, 15*, 1360–1367.

Selim, H. M., Davidson, J. H., & Mansell, R. S. (1976). Evaluation of a two site adsorption desorption model for describing solute transport in soils. In *Proceedings summer computer simulation conference* (pp. 444–448), Washington D.C.

Sparks, D. L. (1989). *Kinetics of soil chemical processes*. San Diego: Academic Press.

Tunega, D., Haberhauer, G., Gerzabek, M. H., & Lischka, H. (2000). Interaction of acetate anion with hydrated Al^{3+} cation: A theoretical study. *The Journal of Physical Chemistry A, 104*, 6824–6833.

Vogt, P. F., & Geralis, J. J. (1985). Aromatic amines. In: *Ullmann´s encyclopedia of industrial chemistry*, vol. A 2 (pp. 37–56). Weinheim: VCH.

Wang, X., Sun, C., Gao, S., Wang, L., & Shuokui, H. (2001). Validation of germination rate and root elongation as indicator to assess phytotoxicity with Cucumis sativus. *Chemosphere, 44*, 1711–1721.

Weber, E. J., Spidle, D. L., & Thorn, K. A. (1996). Covalent binding of aniline to humic substances. 1. Kinetic studies. *Environmental Science & Technology, 30*, 2755–2763.

Zachara, J. M., Ainsworth, C. C., Cowan, C. E., & Thomas, B. L. (1987). Sorption of binary mixtures of aromatic nitrogen heterocyclic compounds on subsurface materials. *Environmental Science & Technology, 21*, 397–402.

Zeldovich, Y. (1934). The catalytic oxidation of carbon monoxide on manganese dioxide. *Acta Physicochimica U.R.S.S, 1*, 449–464.